

## Extended photoionization and photodissociation in Sgr B2

J.R. Goicoechea<sup>\*1</sup>, N.J. Rodríguez-Fernández<sup>\*\*2</sup>, and J. Cernicharo<sup>\*\*\*1</sup>

<sup>1</sup> Departamento de Astrofísica Molecular e Infrarroja, IEM/CSIC, Serrano 121, E-28006 Madrid, Spain

<sup>2</sup> Observatoire de Paris - LERMA. 61, Av. de l'Observatoire, 75014 Paris, France

Received 7 November 2002, revised 30 November 2002, accepted 2 December 2002

Published online 3 December 2002

**Key words** Galaxy: center — infrared: ISM: lines and bands — ISM: dust, extinction—HII regions — ISM: individual (Sagittarius B2)

**PACS** 04A25

We present large scale  $9' \times 27'$  ( $25 \text{ pc} \times 70 \text{ pc}$ ) far-IR observations of the Sgr B2 complex using the spectrometers on board the *Infrared Space Observatory*<sup>1</sup> (ISO). The far-IR spectra are dominated by the strong continuum emission of dust and by the fine structure lines of high excitation potential ions (NII, NIII and OIII) and those of neutral or weakly ionized atoms (OI and CII). The line emission has revealed a very extended component of ionized gas. The study of the NIII  $57 \mu\text{m}$ /NII  $122 \mu\text{m}$  and OIII  $52 \mu\text{m}$  /  $88 \mu\text{m}$  line intensity ratios show that the ionized gas has a density of  $n_e \simeq 10^{2-3} \text{ cm}^{-3}$  while the ionizing radiation can be characterized by a diluted but hard continuum, with effective temperatures of  $\sim 35000 \text{ K}$ .

Photoionization models show that the total number of Lyman photons needed to explain such an extended component is approximately equal to that of the HII regions in Sgr B2(N) and (M) condensations. We propose that the inhomogeneous and clumpy structure of the cloud allows the radiation to reach large distances through the envelope. Therefore, photodissociation regions (PDRs) can be numerous at the interface of the ionized and the neutral gas. The analysis of the OI ( $63$  and  $145 \mu\text{m}$ ) and CII ( $158 \mu\text{m}$ ) lines indicates an incident far-UV field ( $G_0$ , in units of the local interstellar radiation field) of  $10^{3-4}$  and a H density of  $10^{3-4} \text{ cm}^{-3}$  in such PDRs. We conclude that extended photoionization and photodissociation are also taking place in Sgr B2 in addition to more established phenomena such as widespread low-velocity shocks.

### 1 Introduction

The Sgr B2 complex represents an interesting burst of massive star formation in the inner 400 pc of the Galaxy (that we refer as the Galactic Center region [GC]) and may be representative of other active nuclei. Large scale continuum emission studies show that Sgr B2 is the brightest emission and the most massive cloud of the region ( $\simeq 10^7 M_\odot$ ; Lis & Goldsmith 1989). The main signposts of star activity are located within three dust condensations labelled as Sgr B2(N), (M) and (S). They contain all the tracers of on-going star formation: ultracompact HII regions driven by the UV field of newly born *OB* stars, hot cores embedding proto-stars, molecular masers and high far-IR continuum intensity. These *core* regions are surrounded by a low density ( $n_{H_2} \leq 10^4 \text{ cm}^{-3}$ ) extended envelope ( $\sim 15'$ ), hereafter Sgr B2 envelope, of warm gas ( $T_k \geq 200 \text{ K}$ ) and cool dust ( $T_d = 20\text{--}30 \text{ K}$ ; Hüttemeister et al. 1995). A summary of the different components present in Sgr B2 and their main characteristics is shown in figure 1 [*left*].

The origin of the observed rich chemistry in the Sgr B2 envelope and its possible heating mechanisms are far from settled and several scenarios have been proposed. Low-velocity shocks have been traditionally

\* Corresponding author: e-mail: javier@isis.iem.csic.es, Phone: +0034 91 561 68 00, Fax: +0034 91 564 55 57

\*\* e-mail: Nemesio.Rodriguez-Fernandez@obspm.fr

\*\*\* e-mail: cerni@astro.iem.csic.es

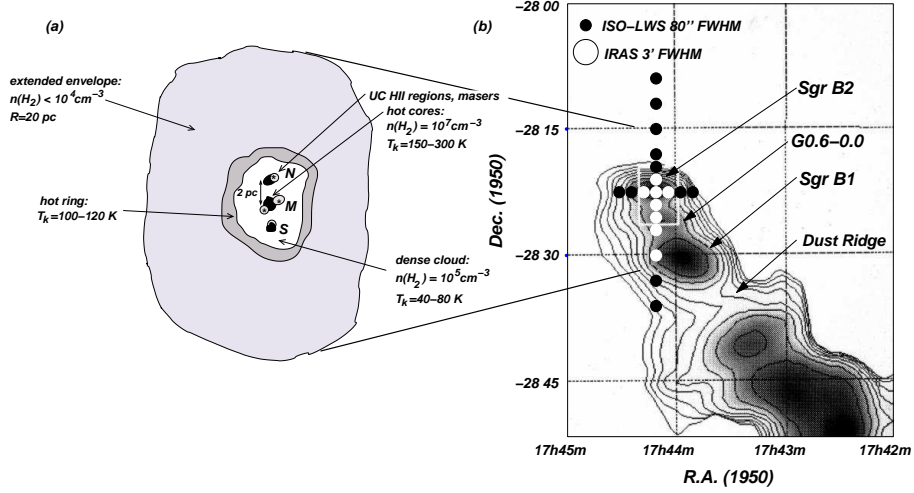


**Fig. 1** *Right* : Large scale IRAS image at  $60 \mu\text{m}$  (Gordon et al. 1993) and ISO target positions across Sgr B2 region. *Left* : Sketch showing the different structures and components in the Sgr B2 complex. Hot cores are shown black shaded and HII regions are the structures enclosing the stars. (Adapted from Hüttemeister et al. 1995)

invoked to explain the enhanced abundances of SiO or  $\text{NH}_3$  and the differences between gas and dust temperatures (cf. Flower et al. 1995). The origin of shocks in the Sgr B2 envelope have been associated either with large scale cloud–cloud collisions or with small scale wind–blown bubbles produced by evolve massive stars (Martín–Pintado et al. 1999).

The effect of the UV radiation in the Sgr B2 envelope has been traditionally ruled out because of the gas and dust temperature differences, the unusual chemistry and the absence of thermal radio-continuum and ionized gas outside the HII regions and hot cores within the central condensations. Our observations reveal the presence of an extended component of ionized gas detected by fine structure emission.

All this new data suggest that UV radiative–type processes are also important in the heating of the GC gas in addition to mechanical mechanisms, as can be in other GC clouds (see Rodríguez-Fernández et al. 2003). In this contribution we present a brief summary of the results obtained by ISO<sup>1</sup> in the Sgr B2 envelope (Fig. 1 [*right*]) concerning the ionized gas and the effects of the UV radiation.

## 2 Extinction corrections

The large  $\text{H}_2$  column density (up to  $10^{25} \text{ cm}^{-2}$ ) found in Sgr B2 suggests that even in the far-IR, fine structure lines can suffer appreciable reddening. We have estimated the prevailing extinction in each position by converting the continuum opacity into visual extinction. The spectra can not be fitted with a single gray body. Thus, we have modeled the observed continuum spectrum as a sum of two gray bodies. The total continuum flux in the model is:

$$S_\lambda = (1 - e^{-\tau_\lambda^{\text{warm}}}) B_\lambda(T_{\text{warm}}) \Omega_{\text{warm}} + (1 - e^{-\tau_\lambda^{\text{cold}}}) B_\lambda(T_{\text{cold}}) \Omega_{\text{cold}} \quad (1)$$

where  $B_\lambda(T_i)$  is the Planck function,  $\tau_\lambda^i$  is the continuum opacity and  $\Omega_i$  is the solid angle subtended by the  $i$  dust component. The continuum opacity is given by  $\tau_\lambda = 0.014 A_V (30/\lambda)^\beta$  where  $\beta$  is the grain emissivity exponent of each dust component. The observed spectral energy distributions are best fitted with a dust component with a temperature of 13–22 K and a warmer component with a temperature of 24–39 K.

<sup>1</sup> Based on observations with ISO, an ESA project with instruments funded by ESA Member States (especially the PI countries: France, Germany, the Netherlands and the United Kingdom) and with participation of ISAS and NASA.

The warmer component contribute in less than 10 % to the total optical depth. The higher dust temperatures are those measured in the southern part of Sgr B2. Depending of the position, the derived extinction varies from  $\sim 20$  to  $\sim 1000$  magnitudes (see table 1 for lower and upper limits to the visual extinction).

### 3 The ionized gas

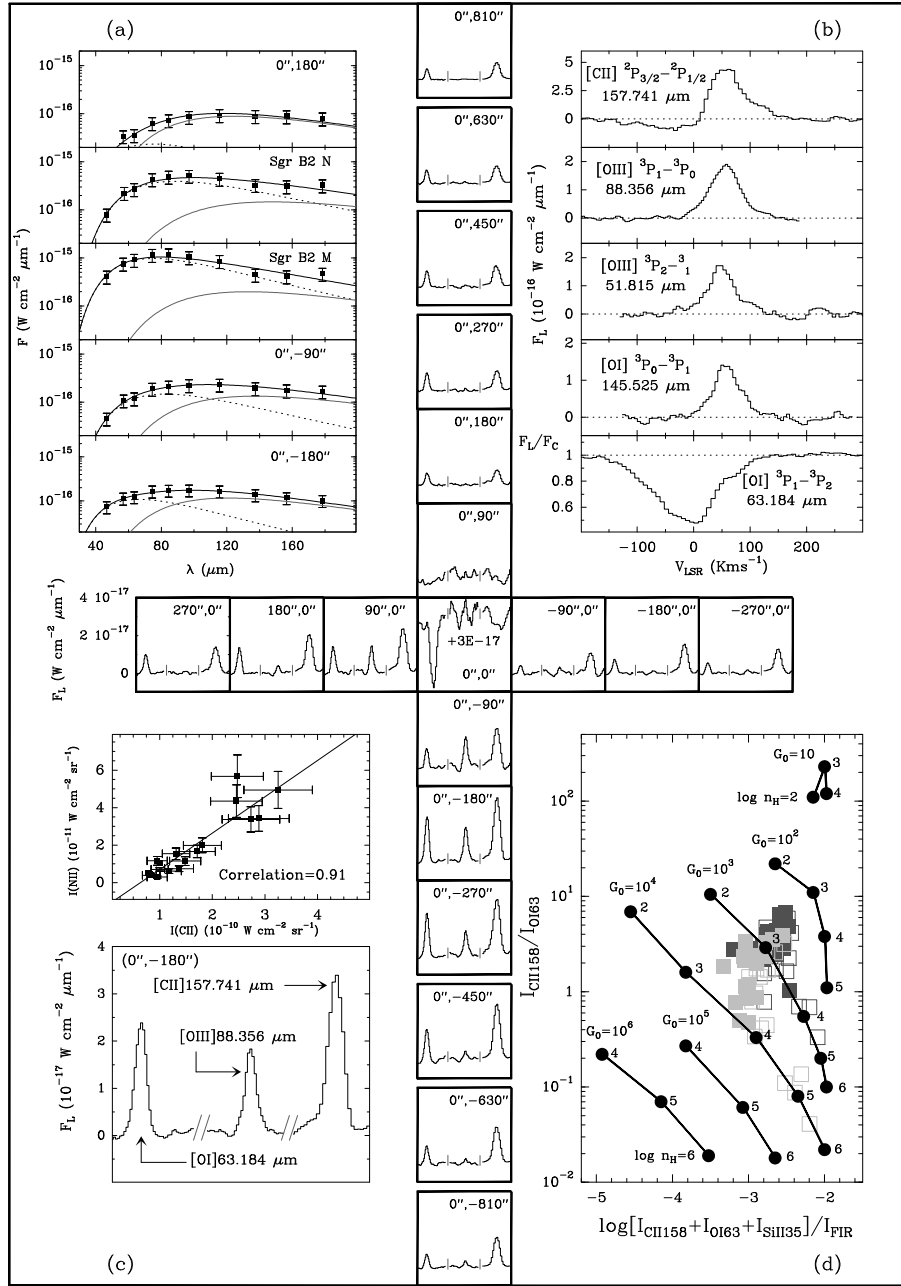
The far-IR spectra exhibit several fine structure lines from the ionized material. We have clearly detected the [OI]63 and 145  $\mu\text{m}$ , and [CII]158  $\mu\text{m}$  lines in all observed positions. In addition, lines coming from the [NII]122  $\mu\text{m}$ , [NIII]57  $\mu\text{m}$  [OIII]52 and 88  $\mu\text{m}$  lines are also detected in most positions, revealing a prominent component of ionized gas in the southern and eastern regions of Sgr B2.

Table 1 lists the extinction corrected OIII 52/88 line intensity ratios for the two derived limits to the extinction across the region. For extended emission sources and lines excited by collisions with electrons (see Rubin et al. 1994) we derive electron densities ( $n_e$ ) in the range  $\simeq 10^{2-3} \text{ cm}^{-3}$  for the extended envelope. At the limited spectral resolution of the LWS/grating mode, OIII lines are hardly detected in the central positions. Nevertheless, Fig. 2b shows their Fabry-Perot detection in Sgr B2(M). Both OIII lines appear centered at  $V_{LSR} \simeq 50 \pm 15 \text{ km s}^{-1}$  and do not show emission/absorption at more negative velocities (foreground gas). Considering  $A_V > 1000$  magnitudes, we found  $n_e \geq 10^{5.5} \text{ cm}^{-3}$  in Sgr B2(M).

Table 1 also lists the extinction corrected NIII57/NII122 line intensity ratios. The minimum averaged ratio is  $\sim 0.77$  while the upper limits are dependent to the maximum extinction affecting the lines. For those ratios, we derive minimum effective temperatures ( $T_{eff}$ ) for the ionizing radiation of 32000 – 36000 K. Those  $T_{eff}$  should be considered as a lower limit to the actual  $T_{eff}$  of the ionizing source if this is located far from the nebular gas. We have carried out CLOUDY (Ferland 1996) simulations showing that the observed line ratios are consistent with an scenario where almost all ionizing photons arise from the HII regions within Sgr B2(M) and (N). The total flux of Lyman continuum photons is  $10^{50.3} \text{ s}^{-1}$  and  $T_{eff} = 35000 \text{ K}$ . The differences in the observed NIII/NII ratios are due to the dilution of the incident radiation (lower ionization parameter). Hence, the size of the ionized region can only be explained if the medium is highly inhomogeneous. This suggests that the clumpy nature of the cloud allows the radiation to reach large distances through the envelope. In this scenario, several PDRs can be expected in the interface between the ionized and the neutral gas.

**Table 1** Selected line ratios after correcting for the estimated minimum and maximum extinction. The different beam sizes of each LWS detector are taken into account and extended emission is considered. Offsets are in arcsec.

map position	warm dust $A_V$ (mag)	cold dust $A_V$ (mag)	OIII R(52/88)	$n_e$ (OIII) $\log(\text{cm}^{-3})$	NIII/NII R(57/122)	$T_{eff}^{min}$ ( $\div 10^3 \text{ K}$ )
(0,810)	1.2-1.5	15-55	<2.40	<3.18	<0.72	<33.2
(0,630)	1.6-2.0	23-84	1.79-2.23	2.83-3.10	<0.72	<33.2
(0,450)	1.1-1.8	25-92	1.36-1.73	2.49-2.79	<0.26	<31.8
(0,270)	5.2-8.0	41-112	<1.61	<2.70	<1.77	<35.6
(0,180)	0.7-1.7	131-294	<3.55	<3.66	<2.73	<35.2
(0,-90)	16-18	367-877	1.27-8.11	2.41-4.67	1.60-11.3	(35.0-37.2)
(0,-180)	3.7-5.2	148-493	0.90-3.18	1.99-3.53	0.78-2.95	(34.9-35.3)
(0,-270)	2.8-3.8	59-205	0.41-0.69	1.03-1.67	0.79-1.39	(35.0-35.8)
(0,-450)	2.7-3.2	28-102	1.14-1.50	2.28-2.61	0.18-0.24	(31.6-32.2)
(0,-630)	3.5-3.9	23-85	1.83-2.30	2.85-3.13	0.55-0.71	(32.9-33.2)
(0,-810)	1.1-1.3	16-59	0.55-0.64	1.39-1.58	0.18-0.21	(32.8-33.1)
(270,0)	27-28	156-536	<1.19	<2.24	<3.13	<36.6
(180,0)	4.9-6.6	78-276	1.14-2.38	2.28-3.18	<0.95	<33.6
(90,0)	7.4-9.0	168-565	0.62-2.64	1.53-3.30	1.31-6.07	(35.7-36.3)
(-90,0)	28-34	228-579	0.85-2.97	1.92-3.44		
(-180,0)	21-26	62-168	0.43-0.63	1.10-1.55		
(-270,0)	21-25	45-124	0.38-0.50	0.94-1.27		



**Fig. 2** ISO/LWS-grating mode raster map of the [OI]63, [OIII]88 and [CII]158  $\mu\text{m}$  lines. Offset positions are given in arcsec respect to Sgr B2(M) ( $0'', 0''$ ). (a) Averaged continuum flux of each ISO/LWS detector and gray-body best fits for some selected positions. The error bars correspond to a 30 % of flux uncertainty. (b) Fine structure lines detected with ISO/LWS-FP mode in Sgr B2(M). (c) *[Top]* Correlation between the [NII]122  $\mu\text{m}$  and [CII]158  $\mu\text{m}$  lines. SgrB2(M) and (N) are not included. *[Bottom]* Main features of the grating raster map labelled. (d) CII/OI intensity ratio vs. (CII+OI+SiII)/FIR for several PDR models of varying FUV fields and hydrogen densities (from Wolfire et al. 1990). The space parameter occupied by Sgr B2 envelope is represented by gray squares (see text).

## 4 The Photodissociation regions

The large OH column density of warm ( $T_k \simeq 300$  K) and low density gas ( $n_{H_2} \leq 10^4$  cm $^{-3}$ ) recently found in the envelope of Sgr B2 suggested that its external shells are illuminated by a strong far-UV field that photodissociate the large amount of water vapor found in the region (Goicoechea & Cernicharo 2002). However, the main properties of the associated warm PDRs could not be derived. For that purpose, we have compared the far-IR continuum emission, and the [CII] 158, [OI]63 and 145  $\mu$ m lines at each position with PDR theoretical models. Figure 2d shows our results in comparison with predictions from PDR models of Wolfire, Tielens and Hollenbach (1990). The gray squares show the parameter space occupied by the Sgr B2 positions for intensity ratios corrected for the minimum (filled) and maximum (not filled) visual extinction estimated from the continuum analysis. The observational points scatter around a far-UV flux,  $G_0$ , of  $\simeq 10^{3-4}$  and  $n_H \simeq 10^{3-4}$  cm $^{-3}$  depending on the use of all observed CII flux (dark gray) or the remaining CII flux after subtracting the CII emission arising in (non-PDR) low-density ionized gas and correlated with the NII emission. From the observed correlation (see Fig. 2c) we estimate that 20 to 70 % of the CII emission arises in the PDRs of Sgr B2. In addition, both the observed [CII]158/[OI]63 and ([CII]158+[OI]63)/FIR intensity ratios shown in Fig. 2d are not predicted by shocked gas models (Hollenbach & McKee 1989) while they are commonly reproduced in PDR models.

## 5 Summary and perspectives

We have presented new far-IR observations of the Sgr B2 region that reveal a new perspective of the less known extended envelope of the complex. The ISO data show the presence of a widespread component of ionized gas reaching very large distances from the HII regions of known massive star formation. Molecular tracers and atomic fine structure tracers do not show evidences of high-velocity shocks. Hence, the ionized gas can not be explained in terms of high-velocity dissociative shocks. It seems that the well established widespread low-velocity shocks are not the only mechanism heating the gas to temperatures larger than those of the dust. We now have proofs showing that low-velocity shocks and large scale radiative processes, such as the photoelectric effect, coexist in the whole Sgr B2 envelope, difficulting the interpretation of the astronomical data but providing one of the richest and peculiar clouds in the galaxy. Coexistence of mechanical and radiative-type heating mechanisms based on the effects of a far-UV field that permeates an inhomogeneous and clumpy medium seems to be the rule in the envelope of Sgr B2 and in the bulk of GC clouds observed by ISO (Rodríguez-Fernández et al. 2003).

**Acknowledgements** We thank J. Martín-Pintado for stimulating discussions about Sgr B2 and the Galactic Center, and M.A. Gordon for providing us the IRAS maps of Sgr B2. NJR-F has been supported by a Marie Curie Fellowship of the European Community program "Improving Human Research Potential and the Socio-economic Knowledge base" under contract number HPMF-CT-2002-01677.

## References

- [1] Lis, D.C., & Goldsmith, P.F. 1989, ApJ, 337, 704
- [2] S. Hüttemeister, S., Wilson, T.L., Mauersberger, R., Lemme, C., Dahmen G., & Henkel, C. 1995, A&A, 294, 667
- [3] Ferland, G.J. 1996, A Brief Introduction to Cloudy, U. Kentucky, Dept. Physics and Astronomy Internal Report
- [4] Flower, D.R., Pineau des Forêts, G., & Walmsley, M.C. 1995, A&A 294, 815
- [5] Hollenbach, D. & McKee, C.F. 1989, ApJ, 342, 306
- [6] Martín-Pintado, J., Gaume, R.A., Rodríguez-Fernández, N.J., de Vicente P., & Wilson, T.L. 1999, ApJ, 519, 667
- [7] Rubin, R.H., Simpson, J.P., Lord, S.D., et al., 1994, ApJ, 420, 772
- [8] Goicoechea J.R., & Cernicharo, J. 2002, ApJ, 576, L77
- [9] Rodríguez-Fernández N, Martín-Pintado, J., Fuente A., Wilson T.L., 2003, these proceedings
- [10] Wolfire, M.G., Tielens A. G. G. M., & Hollenbach, D. 1990, ApJ, 358, 116